Late-acting self-incompatible system, preferential allogamy and delayed selfing in the heteromorphic invasive populations of *Ludwigia grandiflora* subsp. *hexapetala*

Luis O. PORTILLO LEMUS[1], Marilyne HARANG[1], Michel BOZEC[1], Jacques HAURY[1], Solenn STOECKEL[2], Dominique BARLOY[1]

Short title: Breeding system in a European invasive *Ludwigia*

[1] DECOD, (Ecosystem Dynamics and Sustainability), Institut Agro - Agrocampus Ouest, IFREMER, INRAE, Rennes, France

[2] IGEPP, INRAE, Institut Agro, Univ Rennes, 35653, Le Rheu, France

Corresponding author: Dominique.Barloy@Agrocampus-Ouest.fr

Orcid number:

Luis O. PORTILLO LEMUS: 0000-0003-2123-4714

Jacques HAURY: 0000-0002-8628-8265

Solenn STOECKEL: 0000-0001-6064-5941

Dominique BARLOY: 0000-0001-5810-4871

Abstract

Breeding system influences local population genetic structure, effective size, offspring fitness and functional variation. Determining the respective importance of self- and cross-fertilization in hermaphroditic flowering plants is thus important to understand their ecology and evolution. The worldwide invasive species, *Ludwigia grandiflora* subsp. *hexapetala* (*Lgh*)

presents two floral morphs: one self-compatible short-styled morph (S-morph) and one self-incompatible long-styled morph (L-morph). In this study, we identified the breeding systems of western European experimental and natural populations of *Lgh* by comparing structural characteristics of pollen and style, by studying self- and cross-pollen tube elongations and the viability of the resulting seeds and seedlings in both floral morphs. Our results showed no differences in pollen shape and stigma surfaces among and between the two floral morphs. In the self-incompatible L-morph flowers, self-pollen tubes were stopped tardily, in the ovarian area, and were unable to fertilize the ovules. This first formal identification of a late-acting, prezygotic self-incompatible system in *Ludwigia* genus questions on the distribution of this breeding system in the Myrtales order. In the self-compatible S-morph flowers, self-pollen always succeeded to self-fertilize the ovules that nearly all developed into viable seedlings. However, cross-pollen tubes always elongated faster than self-pollen tubes. S-morph individuals may thus advantage preferential allogamy over selfing when cross-pollen is available despite its self-compatibility. As expected in late-acting self-incompatible systems, L-morph flowers authorised 0.2‰ of selfed seeds during the uppermost flowering season, that increased to 1‰ at the end of the flowering season. Such delayed selfing resulted in a significant quantity of viable floating seeds. They may contribute to the local regeneration, seed bank and propagation of the L-morph, which may contribute to explain its invasion success worldwide. Management plans of *Lgh* would gain to consider the breeding systems we identified.

Keywords: Delayed selfing, Mating system, Onagraceae, Pollen tube elongation, Self-fertilization, Water primrose

Introduction

Around 50% of angiosperm species develop a variety of self-incompatible mechanisms that favour allogamy by avoiding self-fertilisation and promoting outcrossing (Igic et al. 2008; Fujii et al. 2016). Self-incompatibility (SI) is the inability of functional male and female gametes to achieve self-fertilization and fertilization in particular combinations of parents. Prezygotic SI involve biochemical reactions resulting from the pollen-pistil interaction that blocks incompatible pollen before sperm fertilizes an egg. Out of a handful of model species, the precise nature of these reactions in most species is not clearly understood, with an intriguing paradox: recurrent patterns of SI are ubiquitous across families but with a large diversity in the type of sites of reaction (Charlesworth et al. 2005; Allen and Hiscock 2008; Shimizu and Tsuchimatsu 2015). Characterizing the type of SI individuals develop in a species by identifying the site of the incompatible pollen-pistil rejection is a first essential step to understand and predict how its breeding system may shape the evolution of its populations in their ecological contexts (Charlesworth et al. 2005; Takayama and Isogai 2005; Busch and Schoen 2008; Ferrer and Good 2012; Grossenbacher et al. 2017). Moreover, characterizing the prevalence of SI systems developed in species, genera and families across the Angiosperms and eucaryotes contribute understanding which biological, ecological and evolutionary features may explain the ubiquitous occurrence of mechanisms favouring allogamy across the tree of life (Charlesworth et al. 2005; Igic et al. 2008; Santos-Gally et al. 2013; Gibbs 2014; Fujii et al. 2016; Grossenbacher et al. 2017; Barrett 2019). Breeding systems are indeed the main factor influencing the evolution of genetic diversity in populations and species with potential consequences for adaptation and speciation (Duminil et al. 2007; Ellegren and Galtier 2016).

We currently consider three major mechanisms of SI in flowering plants, homomorphic gametophytic, homomorphic sporophytic and heteromorphic sporophytic, that differ in the site of the rejection of incompatible pollen tubes (Gibbs and Bryan 1986; Dickinson et al. 1992;

70 Hinata et al. 1993; Barrett and Cruzan 1994; Kao and McCubbin 1996; de Nettancourt 1997).
71 Homomorphic SI systems imply that flowers with different SI types present the same flower
72 shape and structure, or a continuous variation of floral morphologies not correlated with
73 compatibility. By contrast, heteromorphic self-incompatibility (HetSI) associates different
74 compatibility between individuals with different floral morphologies, sometimes associated
75 with additional features such as different patterns of spatial separation of anthers and stigmas
76 (Webb and Lloyd 1986; Opedal 2018), differences in pollen sizes and shapes, and different
77 lengths of stigmatic papillae (Darwin 1877; Barrett and Shore 2008; Igic et al. 2008; Barranco
78 et al. 2019; Barrett 2019; Matsui and Yasui 2020). Commonly, species with style polymorphism
79 have a sporophytic heteromorphic (*i.e.,* di- or tri-allelic) incompatibility system that prevents
80 self-fertilization and crosses between individuals of the same floral morph (Barrett 2019).

81 In most studied species developing these three SI systems, pollen-tube growth is stopped
82 from the stigma or in the style as a result of a rapid response to the pollen–pistil interaction.
83 However, some species present a delayed reaction of self-pollen rejection, named ovarian or
84 late-acting self-incompatibility (LSI) because occurring lately in the ovarian area (Seavey and
85 Bawa 1986; Gibbs and Bianchi 1993; Sage et al. 1994; Gibbs 2014). It often coincides with a
86 residual permeability of their SI systems resulting in a steady low level of selfing despite an
87 effective late-acting SI (Seavey and Bawa 1986; Gibbs 2014). It concerns both homomorphic
88 and heteromorphic species (Gibbs 2014; Simon-Porcar et al. 2015). For example, the
89 homomorphic LSI Theaceae species *Camelia oleifera* and *Camelia sinensis,* allow 10% and
90 ~2% of self-fertilization resulting in viable seeds, respectively (Chen et al. 2012; Liao et al.
91 2014). In the ovarian LSI heteromorphic *Narcissus spp.* from the Amarilidacea, from 4 to 30%
92 of their seed-sets result from self-fertilization (Barrett et al. 2004; Medrano et al. 2012; Simon-
93 Porcar et al. 2015). Within pre-zygotic LSI, Gibbs (2014) proposes to distinguish LSI
94 mechanisms stopping pollen tubes before ovaries (as found in *Melaleuca spp*. and *Thryptomene*

95 *calycina,* Barlow and Forrester 1984; Beardsell et al. 1993) from those stopping self-pollen
96 tubes while penetrating the ovules (as found in *Acacia retinodes,* Kenrick et al. 1986).

97 In the *Ludwigia* genus (Onagraceae), 8 of 82 species have been reported as "self-
98 incompatible", although the nature of their SI were not formally studied and established (Raven
99 1979). The water primrose*, Ludwigia grandiflora* subsp. *hexapetala* (Hook. & Arn.) Nesom
100 and Kartesz (2000), (hereafter *Lgh*), is one of the most invasive aquatic plants in the world,
101 currently spreading out of South America into North America, Europe and Eastern Asia (EPPO
102 2011, Thouvenot et al. 2013; Portillo-Lemus et al. 2021). Tackling how this species reproduces
103 is crucial for understanding its expansion and alleviate its impacts in aquatic environments
104 (EPPO 2011). Yet, we still don't know how sexual reproduction works in this invasive species
105 (Dandelot 2004; Ruaux 2008; Thouvenot et al. 2013). *Lgh* presents two types of floral
106 morphologies in European populations: a short-styled morph (S-morph) that is self- and intra-
107 morph compatible (crosses produce viable seeds), and a long-styled morph (L-morph) that is
108 self- and intra-morph incompatible (crosses do not produce seeds, Portillo-Lemus et al. 2021).
109 In both floral morphs, inter-morph crosses always produce viable seeds. The two floral morphs
110 of *Lgh* develop bowl-shaped non-tubular flowers with two whorls of stamens of different
111 heights. In the L-morph flowers, stamens of the second whorl (inner whorl) are longer than
112 these of the first whorl (outer whorl). These two characteristics contrast with typical
113 heteromorphic SI species that most frequently present tubular flowers and only one whorl of
114 stamens (Barrett and Shore 2008; Cohen 2010; Barrett 2019). Interestingly, floral morphs are
115 mostly found in allopatric monomorphic populations (*i.e.,* exclusively S-morph or exclusively
116 L-morph populations) in Western Europe and other invasive worldwide populations (Hieda et
117 al. 2020; Portillo-Lemus et al. 2021). Surprisingly, around 75% of the invasive populations
118 worldwide seem exclusively composed of self-incompatible L-morph individuals, tackling the
119 paradigm that successful invasive species may be mostly composed of individuals able to

120 reproduce using self-fertilization when mating (Baker 1955; Cheptou 2012; Razanajatovo et al.
121 2016). Recently, some isolated monomorphic L-morph self-incompatible populations were
122 however found to produce seeds (Portillo-Lemus et al. 2021). These puzzling observations
123 question the type of SI reaction involved in the self-incompatible L-morph and its level of
124 permeability to self -fertilization. More broadly, they question the type of breeding systems
125 developed in these invasive populations (Hieda et al. 2020; Portillo-Lemus et al. 2021).

126 In this study, we thus aimed at better characterizing the breeding system of the two floral
127 morphs in Western European populations of *Lgh* by tracking the fates of self- and inter-morph
128 pollen tubes in both floral morphs. First, we searched for structural evidences through analysis
129 of the morphologies of pollen grains and stigma surfaces of the two floral morphs that may be
130 characteristic of homomorphic and heteromorphic sporophytic self-incompatibilities. Second,
131 to better categorize the type of the SI developed by this species, we aimed at identifying the site
132 where the incompatible pollen tubes were blocked in the self-incompatible L-morph pistils. To
133 achieve this goal, we followed the germination and the progression of the self- and inter-morph-
134 pollen tubes on histological sections, prepared at different times after pollination. Third, to
135 quantify the permeability of this self-incompatible system, we counted the number of viable
136 seeds and seedlings obtained from self-fertilization in controlled conditions and in natural
137 monomorphic L-morph populations. Fourth, to test if the S-morph individuals truly reproduced
138 using selfing, as expected in this self-compatible morph, we followed the progression of the
139 self- and inter-morph-pollen tubes, as described for the morph-L, and studied the viability of
140 obtained seeds and seedlings. Finally, we discuss on the contribution of the patterns of SI
141 reactions and breeding system found in *Lgh* with those already observed in other species, with
142 a special focus on the Myrtales order that includes the *Ludwigia* genus.

143

144 # Materials and Methods

145 ## Plant material and sampled populations

146 To better characterize the breeding system of the two floral morphs that were previously
147 reported in *Lgh*, (Portillo-Lemus et al. 2021), we studied a total of 100 individuals growing
148 along the Loire valley in France (Table S1 for GPS location). We sampled five monomorphic
149 populations only composed of S-morph individuals (distance between them: min=40km,
150 mean=146km, max=301km) and five monomorphic populations only composed of L-morph
151 individuals (distance between them: min=6km, mean=124km, max=274km). In each
152 population, we randomly sampled 10 stems per population. *Lgh* partly reproduce using clonal
153 budding and rhizomes (Thouvenot et al 2013). We also know using allele sharing distances
154 between pairs of individuals from 30 individuals genotyped using 38 polymorphic SNPs that,
155 at least in one of these monomorphic populations (Mazerolle), populations present different
156 genotypes within a same floral morph though with a restricted number of ancestors (Genitoni
157 et al. 2020). Sampled stems of all S-morph and L-morph populations were transplanted into a
158 common greenhouse (location: L'institut Agro, Rennes, France. 48°06'47.7"N 1°42'30.2"W)
159 where individuals from one population were growth together in an 80L container to avoid
160 environmental influences on pollen shapes, pollen tube elongations, ovule and seed
161 developments. The 10 containers were watered every 15 days with a commercial nutrient
162 solution (6% nitrogen, 6% phosphorus and 6% potassium) during growth and flowering periods
163 to avoid nutritional deficiencies.

164

165 **Measure of herkogamy**

166 To link breeding systems with floral morphs, we measured the spatial separation on a vertical
167 axis of anthers and stigmas within flowers (herkogamy) from the 10 *Lgh* populations we
168 sampled, as this floral trait would have a negative relationship with the rate of autofertility in
169 plant species (Webb and Lloyd 1986). Herkogamy is usually quantified as the difference
170 between pistil and stamen lengths (respectively, $x_{♀}$ and $x_{♂}$) with their natural twists and
171 curvatures (Opale 2018). Flowers with stigmas positioned above or protruding beyond the
172 anthers would have higher probability to be contacted first by a visiting pollinator which
173 corresponds to approach herkogamy. Flowers in which anthers are above the pistil and with
174 higher probability to be contacted first by pollinators which corresponds to reverse herkogamy.
175 *Lgh* flowers present two whorls of stamens. We thus did 150 measures, i.e., the length of the
176 pistil ($x_{♀}$) and the length of the inner ($x_{♂i}$) and outer ($x_{♂o}$) stamens per floral morph, and
177 calculate difference between length of pistil and length of anther.

178

179 **Histological preparations**

180 To observe pollen and stigmatic papillae morphology, to follow pollen tube growth and to
181 achieve histological sections of ovaries for studying embryo development, we fixed flowers in
182 FAA 1: 2: 20 (formalin: acetic acid: ethanol V/V). Pollen germination, pollen tube growth and
183 ovule penetration were observed using the aniline blue fluorescence method (Martin 1959). The
184 fixed samples were washed several times with distilled water and each flower was placed in
185 1mL of staining solution (0.1% w/v aniline blue, 1% v/v tween-20$^{(R)}$, 0.2 M K_2PO^4, 0.1 M
186 NaOH) for 1 hour at 95°C. After squashing the pistils between the slide and coverslip,
187 observations were made under ultraviolet light (335-364 nm) with a microscope Leica DM4000
188 B$^{©}$, and a camera 190HD. To observe embryo development, fixed ovaries were dehydrated,

189 embedded in paraffin, sectioned at 15 µm with a microtome, and mounted on glass slides (Sakai,
190 1973). Sections were placed in 0.05% toluidine blue O in distilled water for 2–30 min, rinsed
191 once in water for 1 min, and air-dried. Paraffin was removed using two xylene baths and the
192 cover slip was mounted with resin. Histological preparations were realized by Nublat
193 Laboratory (https://www.laboratoire-nublat.com/118botanique.html).

194

195 **Pollen and stigmatic papillae morphologies**

196 To assess if the two floral morphs found in western Europe populations of *Lgh* showed
197 difference in pollen shapes and sizes in association with floral morphs, we studied the shape of
198 500 pollen grains per floral morph. For each morph, we sampled 25 flowers in the 5
199 corresponding populations. For each of these flowers, we measured 20 pollen grains from a mix
200 of the stamen verticels, resulting into a total of 1000 pollen grain measures for both morphs.
201 We measured their diameter under an optical microscope. To assess if S-morph and L-morph
202 flowers of *Lgh* showed difference in stigmatic papillae structure as sometimes found in some
203 heteromorphic SI species, we also noted the long or short shape of stigmatic papillae in 30
204 histological stylar sections for each of the two floral morphs (Dulberger 1992).

205

206 **Pollen tube growth, ovule fertilisation and embryo-sac development**

207 To identify in the self-incompatible L-morph pistil where self-pollen tubes were blocked and
208 to characterize the type of breeding preferentially achieved in the two floral morphs, we
209 performed hand-controlled pollinations to track and compare the self- and inter-morph pollen
210 tube growth in both floral morphs. As experimental pollinations in *Lgh* have previously shown
211 that self- and intra-morph pollinations in L-morph flowers gave similar rates of rejections

212 (Portillo Lemus et al 2021), here we focused our experiments on a comparison between self-
213 pollinations (pollen grains from the same flowers) and reciprocal inter-morph pollinations. To
214 perform controlled self-pollinations, we enclosed early flower buds in cellophane bags to
215 protect them from external pollen. To effect self-pollination, we dissected mature anthers using
216 tweezers to place pollen directly on its own receptive stigma and re-enclosed the flowers in
217 cellophane bags. For reciprocal inter-morph pollination, to simulate free random crosses, we
218 selected five pollen-donor flowers from the other morph to generate a pollen mix. Flowers to
219 receive inter-morph pollen were emasculated before anthesis and then pollinated with this mix
220 of pollen. After pollination, the pollinated flowers were once again enclosed in cellophane bags
221 in order to protect them from any contaminant pollen.

222 To study self- and inter-morph pollen tube growth in both floral morphs, we made 150 self-
223 pollinations per morph and 300 reciprocal inter-morph pollinations between S-morph and L-
224 morph. At 2, 3, 7, 16, 24 hours after the hand-controlled pollination, we randomly sampled and
225 fixed 30 flowers per morph and pollination type. For each flower, pollen tube growth and ovule
226 fertilisation were observed using aniline blue fluorescence method with squashed pistils. We
227 measured the growth of the pollen tubes, *i.e.,* the distance between the stigma and the tip of
228 pollen tube (d, µm) at 2, 3, 7, 16, 24 hours (*t*) after the hand-controlled pollinations. From these
229 measures, we calculated the speed of pollen tube (speed) between two measures in micrometres
230 per hour (µm/h) as $speed = \frac{d_{t_2} - d_{t_1}}{t_2 - t_1}$ and the acceleration of pollen tube growth in micrometres
231 per hour square (µm/h²) as $acceleration = \frac{speed_{t_2} - speed_{t_1}}{t_2 - t_1}$.

232 To evaluate the viability of fertilisation and study the embryo-sac development, we analysed a
233 total of 2520 ovary sections corresponding to 14 sections of five flowers per floral morph and
234 cross type, over nine-time steps (1, 2, 3, 4, 5, 6, 7, 15, 21 days after pollination (*dap*).

235

236 **Fruit and seed set production**

237 To assess the incidence of self-fertilisation in the self-incompatible L-morph individuals, 1600
238 self-pollinations were carried out from July to August (summer), and from September to
239 October (fall), respectively. Self-pollinated L-morph flowers were randomly selected within
240 groups of individuals growing in the greenhouse. As a control, we made 30 self-pollinations
241 with self-compatible S-morph flowers, 30 L x S and 30 S x L-morph pollinations during
242 summer and repeated this sequence during the fall.
243 We also assessed the rate of self-fertilisation in self-incompatible L-morph from *in situ*
244 populations at the beginning of October. We collected the fruits of five S-morph and five L-
245 morph *in natura* populations to evaluate the fruit and seed sets. To quantify the fruit-set *in*
246 *natura*, we counted fruits produced in five quadrats of 1 m^2, 10 m away on a linear transect. As
247 S-morph populations showed a massive fruit production, we estimated the seed-set production
248 per m^2 as the mean number of seeds produced by 25 fruits randomly picked in the quadrats (5
249 fruits per quadrat). As the L-morph *in natura* populations produced few fruits, we collected and
250 counted all the seeds produced in all the fruits found in quadrats. We sowed all the *in-natura*
251 produced seeds in the greenhouse to calculate the germination rate as the number of seedlings
252 over the number of sowed seeds.

253

254 **Statistical analysis**

255 To examine possible differences in pollen tube elongations at each time step (time=[2, 3, 7, 16,
256 24 hours]), and the changes in speed and acceleration of elongations along time in the styles of
257 the two floral morphs considering the four possible types of crosses (cross_types=[S-morph
258 self-pollination; S-morph x L-morph; L-morph self-pollination; L-morph x S-morph]), we used
259 ANOVA (type = III) tests. For each time step, we computed three ANOVA models:

pollen_tube_length~cross_types, speed~cross_types*time and acceleration~cross_types*time. For each test, we verified the homoscedasticity of distributions between groups and the normality of residuals using Shapiro–Wilk's tests. When ANOVAs were significant, we applied Tukey's honestly significant difference (HSD) posthoc comparisons of the means to identify which groups and parameters caused those significant differences. We compared measures of herkogamy between S-morph and L-morph flowers using a Mann-Whitney U test and discussed considering their compatibility and realised breeding systems. All analyses were performed using the stats package in R 4.0.4 software (R Development Core Team, 2014). All results were summarised in the supplementary information table S2.

Results

Measures of herkogamy

The measures of herkogamy (pistil length – stamen length in a same flower, Figure S1) showed that, in the L-morph flowers, the heights of the anthers of the 150 outer and 150 inner measured whorls were, respectively always ($U=22500$, $p<0.001$) and significantly ($U=21050$, $p<0.001$) below the heights of the pistil. In the S-morph flowers, the heights of the anthers of the 150 outer measured whorls were significantly below the heights of the pistil ($U=19930$, $p<0.001$), while the heights of the anthers of the 150 inner measured whorls were all above the heights of the pistil ($U=22500$, $p<0.001$).

Pollen and stigmatic papillae morphologies

Pollen grains were all released in triporate monads and connected to the anthers by viscin threads (Fig.1; a3). In both floral morphs and in all the studied populations, pollen grains were

283 all smooth and had the same sizes ranging from 60 to 95 µm whatever their floral morphs
284 (ANOVA, p-value=0.228, Fig. 1 b3, c3). The styles of both floral morphs had capitate stigmas,
285 which were all wet during anthesis and had stigmatic papillae which were submerged by
286 mucilage (Fig. 1; a1, b1). In both floral morphs, all the 60 longitudinal sections of the stigma
287 receptive surface (30 per morph) showed the same morphology of elongated unicellular papillae
288 (Fig. 1; a2, b2). The only difference we found between styles of floral morphs concerned their
289 lengths: styles of S-morph flowers were significantly wider (2.27mm ± 0.19) and shorter (8.04
290 mm ± 0.19) than those of L-morph flowers (width: 1.53 mm±0.09; length: M=8.97±0.25; p-
291 value<0.001, Fig.1; c1, c2), resulting in a difference of around 1mm between long- and short-
292 style lengths.

293

294 **Pollen tube growth and fertilisation**

295 All pollen grains germinated, elongated down the style (Fig. 2a-c), and reached the ovules 24
296 hours after pollen deposition on stigmas (Fig. 2d-e), in self and inter-morph crosses and
297 independent of the pollen origin. In the self-pollinated L-morph flowers, only six ovules of 300
298 studied (2 %) were penetrated by a pollen tube with pollen tube tips located in the area of the
299 embryo sac (Fig. 2f). Figure 2f shows an ovule surrounded by several pollen tubes, but it is
300 unclear whether any of them have penetrated the micropyle. The other 294 unpenetrated ovules
301 showed tips of pollen tubes with a small bulge, stopped between the ovarian tissues and the
302 beginning of the first cell layers of the ovule integuments and we found no traces of pollen tubes
303 in the area of the embryo sac (Fig. 2d, e). All the 300 L-morph ovules that were cross-pollinated
304 with S-morph pollen were penetrated by pollen tubes 24 hours after pollination. All S-morph
305 ovules were penetrated by one pollen tube 24 hours after self and inter-morph pollinations (Fig.
306 2g).

307

308 **Kinetic elongation of pollen tube**

309 In the styles of both floral morphs, until reaching the ovules, inter-morph pollen tubes
310 outdistanced self-pollen tubes (HDS-test, p-value<0.001; Mean and SD values reported in
311 Table S2; Fig. 3). Significant advances of inter-morph pollen tubes were observed from two
312 hours after pollinations. (Fig. S2a). Speed of elongations of pollen tubes in both morphs quickly
313 increased in the first two hours after germination while penetrating the stigma tissues to reach
314 an elongation of 0.3-0.4 mm/hours all along the style, and then doubled their speed of
315 elongation when entering the ovary area (Fig. S2b, Table S2).

316

317 **Fertilisation and embryo development**

318 In both floral morphs, each locule of the pentacarpellate ovary has 12 ± 2 ovules (Fig. S3). The
319 anatropous and bitegmic ovules were disposed along a single longitudinal axis on placentae
320 (Figs. 4, 5 and S3). The embryo sac (female gametophyte) was an *Oenothera*-type and
321 composed of only 4 cells: 2 synergids and an egg-cell on the micropyle side, and a single polar
322 nucleus in the central cell, matching previous observations made on other *Ludwigia* species and
323 other Onagraceae genera (Fig. 4, 5; Rigakishi 1918; Eyde 1977; Tilquin and de Brouwer 1982;
324 Tobe and Raven 1986).

325 In L-morph flowers, 24 hours after pollination, 98% of self-pollen tubes stopped their
326 elongations, lately, in between the ovarian area and the beginning of the first integuments (Fig.
327 4.a, b). In these figures, the pollen tubes seem to be located before the nucellus-epistase out of
328 the embryo sac and did not succeed to pass the synergids. However, it is always difficult to
329 obtain sections showing all together, the synergids, egg cell and central cell which compromise

330 the possibility to identify precisely where the pollen tube stopped. The embryo sacs found with
331 self-pollen tubes stopped didn't develop and degenerated three days after pollination (Fig. 4.c).
332 In the greenhouse, self-pollinated L-morph flowers abscised three days after pollination which
333 is consistent with the temporality of our histological observations (Fig. 4a). In comparison, the
334 abscission of the unpollinated flowers of L-morphs occurred four days after emasculation, when
335 protected with a cellophane bag. Under aniline blue fluorescence, we observed that 2% of self-
336 pollen tubes (6/300) in L-morph flowers succeeded to reach the embryo sac and that only one
337 self-fecundation event was observed over the 300 self-pollinated L-morph studied ovules from
338 the ovary sections (Fig. 4b).

339 In S-morph, regardless of pollen origin, and in L-morph when inter-morph cross-pollinated, the
340 first cell divisions of the embryos began two to three days after pollination (Fig. 5). From five
341 days after pollination, the nucellus gradually began to disintegrate while the embryo continued
342 to develop and grow. At 15 days, the nucellus disappeared completely, giving way to
343 exalbuminous embryo development, which concluded with a viable seed 45 days after
344 pollination.

345

346 **Fruit production in self-incompatible L-morph**

347 In the greenhouse, during summer, only four very "small fruits" containing one, four, five and
348 nine seeds respectively developed over 1600 studied L-morph flowers that were hand-
349 pollinated with self-pollen only (Fig. 6). Considering that 60 ovules on average were initially
350 available per flower, the rate of self-fertilisation was 0.02% (i.e., 19 seeds from 1600 x
351 60=96000 potential ovules available). In the greenhouse, during the fall, at the end of the
352 flowering season, 25 very "small fruits" containing between one and ten seeds for a total of 98
353 seeds (Fig. 6), gave a rate of self-fertilisation of 0.1% (98 on 96000 potential ovules), thus 5-

354 fold more than obtained in July, during the high fruiting period. All 30 S-morph flowers, which
355 were self-pollinated as a control, developed into 30 fruits containing a total of 1800 seeds, with
356 a constant number of 60 seeds per fruit both in July and September (Fig. 6).

357 To validate the results obtained in experimental conditions, we then assessed the production of
358 "small fruits" in five L-morph and five S-morph *in natura* populations (Table S1). We found
359 between 15 and 35 “small fruits” per m^2 in self-incompatible monomorphic L-morph
360 populations. All the “small fruits” collected *in natura* contained one to 15 seeds per fruit, as we
361 obtained in experimental conditions in greenhouse. We counted a production of 92 to 217 seeds
362 per m^2. In the five self-compatible S-morph populations, we counted 384 to 864 fruits per m^2.
363 On five of these fruits per population, we counted 50 to 70 seeds per fruit, giving an estimation
364 of 19200 to 51840 seeds per m^2 (Table S1). All seeds from “small fruits” obtained in greenhouse
365 and *in natura* germinated, and developed into viable seedlings (Table S1).

366

367 **Discussion**

368 The results we obtained from a common garden and from natural populations showed
369 that both floral morphs found in European invasive populations of *Lgh* reproduced using a
370 mixed breeding system, with mechanisms that may result in the production of allogamous and
371 delayed autogamous viable seeds. Pollen grains and stigma surfaces of both floral morphs
372 showed similar sizes and shapes. In the self-incompatible L-morph flowers with approach
373 herkogamy, self-pollen tubes were only stopped when reaching the ovaries, before penetrating
374 the ovules. These observations argue for a prezygotic ovarian LSI system in L-morph flowers
375 of *Lgh*, corresponding to Gibbs (2014) classification. As commonly observed in this kind of SI
376 system (Seavey and Bawa 1986; Gibbs 2014), a small proportion of self-pollen (0.02%),
377 increasing by a factor of 5 at the end of the flowering seasons, succeeded to fertilize the ovules

378 and to develop into seeds. All these seeds then developed into viable seedlings. In the self-
379 compatible S-morph with reverse herkogamy, self-pollen grains succeeded in fertilizing the
380 embryo-sacs that successfully developed into viable seeds and then into viable seedlings. Yet,
381 in the two *Lgh* floral morphs, inter-morph pollen tubes always elongated faster than self-pollen
382 tubes, which may give advantage to intermorph crosses when intermorph pollen is available.

383

384 **The prezygotic LSI system in *Lgh*: a rare but already observed SI system**

385 In European invasive populations, *Lgh* present two floral morphologies, a long-styled
386 prezygotic late-acting self-incompatible L-morph (approach herkogamy) and a short-styled
387 self-compatible S-morph (reverse herkogamy). LSI systems are not specific to heterostylous
388 species as it was also observed in homomorphic species like in *Ipomopsis aggregate* from the
389 Polemoniaceae (Sage et al. 2006).
390 Many HetSI species present differences in size and shape of pollen and stigmas papillae
391 (Dulberger et al. 1975; Dulberger 1992; Barrett and Shore 2008). Less frequently, as we
392 observed here in European populations of *Lgh*, HetSI species show similar pollen shape and
393 papillae structure between floral morphs, as previously observed in *Turnera joelii* and *Turnera*
394 *scabra* (Turneraceae, Safavian and Shore 2010).
395 Three style-polymorphic LSI Amaryllidaceae species, *Narcissus tazetta* L., *Narcissus triandrus*
396 L. and *Narcissus papyraceus* also present similar pollen shape and papillae structure between
397 floral morphs. However, their LSI systems are not related to the heteromorphy of their flowers,
398 as crosses between individuals of the same floral type are fertile, and only strict self-pollination
399 results into ovarian prezygotic pollen rejection (Dulberger 1964; Sage et al. 1999; Barrett and
400 Shore 2008; Simon-Porçar et al. 2015). In the invasive *Lgh* populations we studied here, the
401 genetic ancestrality between individuals may be limited (Genitoni et al. 2020), and we didn't
402 assess the genetic identity of the individuals we sampled along the 530km west-east transect of

403 the Loire watershed. We were thus not able to identify if the LSI we identified in western
404 European *Lgh* populations would be truly heteromorphic, or as in *Narcissus sp.*,
405 nonheteromorphic.
406 In the order of Myrtales, 76 of 674 species of the Onagraceae family were reported to be self-
407 incompatible (Raven 1979). Two of these species, *Oenothera organensis* and *Oenothera*
408 *rhombipetala*, were formally demonstrated to be self-incompatible by studying their pollen tube
409 progression after self and cross pollinations and were reported to involve a homomorphic GSI
410 system (Emerson 1939; Bali and Hecht 1965). In *Epilobium obcordatum,* another self-
411 incompatible species of the Onagraceae family, most of the self-pollen tubes stopped before
412 entering the embryo sac (Seavey and Carter 1996) and were suspected to mate using an ovarian,
413 LSI system (Seavey and Bawa 1986). However, contrary to our observations in *Lgh*, the rare
414 self-fertilised ovules of *E. obcordatum* present substantial rates of post-zygotic failures (Seavey
415 and Carter 1996).
416 Overall, LSI have been previously reported in two other families of the Myrtales order: in the
417 Myrtaceae family, in *Acca sellowiana* (Finatto et al. 2011), in *Melaleuca alternifolia*
418 (Baskorowati et al. 2010) and in *Eucalyptus globulus* (Pound et al. 2002), and in six *Vochysia*
419 species of the Vochysiaceae family (Oliveira and Gibbs 1994). If confirmed, our results may
420 add a third family of the Myrtales order as developing an LSI system. Together with our results,
421 these observations question a possible wider occurrence of LSI in the Myrtales order.
422

423 **Permeability of LSI L-morph flowers: a delayed selfed mating system?**

424 Our results showed that, despite the LSI developed in the L-morph flowers, self-fertilisation
425 still occurred at a low, stable rate in both experimental and *in natura* populations. This type of
426 breeding system enabling for some self-fertilisation especially at the end of flowering season,
427 named delayed selfing, has been reported in multiple angiosperm species as a recurrent breeding

428 strategy (Lloyd 1992; Sakai 1995; Goodwillie and Weber 2018). In such species, self-
429 pollination is blocked or delayed until the opportunity for outcrossing has passed. Delayed
430 selfing is thought to have evolved in preferentially allogamous species because it would provide
431 some reproductive assurance when populations suffer from the lack of compatible pollen
432 (Goodwillie and Weber 2018; Ruane et al. 2020; Xu 2021).

433

434 **A preferential allogamy breeding system even in the self-compatible S-morph?**

435 Before our study, we expected that individuals of the self-compatible S-morph preferentially
436 mates using selfing (Kerbs et al. 2020). Surprisingly, the elongation dynamics of pollen tubes
437 highlighted another process susceptible to favour allogamy in *Lgh*, even in the self-compatible
438 S-morph. In both floral morphs, inter-morph pollen tubes elongated significantly faster than
439 self-pollen tubes while progressing along the style. This phenomenon has already been
440 described in several species with a LSI mating system, like in *Camellia oleifera* and in
441 *Crotalaria juncea* (Liao et al. 2014; Rangappa Thimmaiah et al. 2018). But faster elongation
442 of inter-morph pollen tubes does not occur in all LSI species. For example, self- and cross-
443 pollen tubes present similar elongation speed in *Aconitum kusnezofii* or *Cyrtanthus breviflorus*
444 (Vaughton et al. 2010; Hao et al. 2012). Further studies should determine whether the advantage
445 of inter-morph pollen tube elongation also applies when flowers are pollinated with a mixture
446 of self and inter-morph pollens in controlled pollinations, as reported in *Campsis radicans*
447 (Bertin et al. 1989) or using paternity analysis on seeds produced after free pollination in *in*
448 *natura* populations that mix the two floral morphs, as reported in *Luculia pinceana* (Zhou et al.
449 2015).

450

451 **Consequences of LSI for invasive populations of *Lgh***

Our results showed that invasive populations only composed of the self-incompatible L-morph still produced few small fruits containing few seeds resulting from self-fertilization, in similar proportions to what we obtained in experimental conditions. If these self-fertilized seeds remained limited in number at the scale of an individual, we estimated from our measures in quadrats that populations in Loire watershed still produced from 92 to 217 seeds per m^2 which can all potentially germinate and resulted into viable seedlings. Delayed selfing in the L-morph *Lgh* populations resulted in a consequential quantity of viable floating seeds that may contribute to their local regeneration, seed bank and dissemination. In the invasion context, individuals capable of self-fertilization or uniparental reproduction can regenerate a new population in the absence of compatible partners (Baker 1955; Barrett et al. 2008). Accordingly, a recent survey on 1,752 angiosperm species showed that selfing ability fosters directly and indirectly alien plant establishment (Razanajatovo et al. 2016). In contrast, 75% of the worldwide *Lgh* invasive populations are monomorphic L-morph self-incompatible populations (Portillo-Lemus et al. 2021) which may constitute an anomaly to 'Baker's Law' (Baker 1955). Our results showed that L-morph individuals certainly mated using a LSI system but also used delayed selfing in European invasive populations, better fitting Baker hypotheses. This breeding system with preferential allogamy and delayed selfing, never described before this study, must be considered for the future management plan of *Lgh* invasive populations.

Beyond a system with a compatible S-morph and a self-incompatible L-morph, that may have suggested simple breeding systems, our study revealed a more complex picture, where the two floral morphs combined different mechanisms that may result in preferential allogamy and delayed selfing. Our results encouraged to explore in more details fertilization in plants to better characterise their breeding systems and their consequences for populations. Concerning *Lgh*, we still lack of a clear picture of the respective importance of its reproductive modes in native and invasive populations worldwide in different ecological contexts, including in these

monomorphic populations found along the recent European invasion front. Genetic marker-based analyses of experimental crosses and parentage analyses in natural populations should help validating the relevance of our first results and clarifying the reproductive modes of both floral morphs and natural populations as recently achieved in two Oleaceae species (Besnard et al. 2020, De Cauwer et al. 2021).

Acknowledgements

We warmly thank Noni Franklin-Tong, Emiliano Mora-Carrera, Antoine Vernay, Juan Arroyo and two anonymous reviewers for their useful comments that helped shaping this manuscript. This research was supported by FEDER funds from Région Centre-Val de Loire and by Agence de l'eau Loire-Bretagne (grant Nature 2045, programme 9025 (AP 2015 9025)). FEDER also financed the doctoral grant of L. Portillo and the technical assistance salary of M. Harang. The authors thank Diane Corbin (FRAPNA Loire - Ecopôle du Forez), and Guillaume Le Roux (Réserve Naturelle Val d'Allier Châtel-de-Neuvre) for making plant material available. We thank the Experimental Unit of Aquatic Ecology and Ecotoxicology (U3E) 1036, Institut national de recherche pour l'agriculture, l'alimentation et l'environnement (INRAE, which is part of the research infrastructure Analysis and Experimentations on Ecosystems-France, for help with the maintenance of plants.

Data availability

Here lien Zenodo

Author Contribution

499 LP and DB designed this project. MH, MB, LP and DB performed all experiments. JH
500 participated in capsule husking. LP, SS and DB analysed data and wrote the manuscript. All
501 authors approved the manuscript.

502

503 **References**

504 Allen AM, Hiscock SJ (2008) Evolution and phylogeny of self-incompatibility systems in
505 angiosperms. In: Self-incompatibility in flowering plants. Springer, pp 73–101

506 Baker HG (1955) Self-compatibility and establishment after'long-distance'dispersal.
507 Evolution 9:347–349

508 Bali PN, Hecht A (1965) The genetics of self-incompatibility in *Oenothera rhombipetala*.
509 Genetica 36:159–171. https://doi.org/10.1007/BF01557151

510 Barlow BA, Forrester J (1984) Variation in indumentum morphology in the *Melaleuca*
511 *leucadendra* complex (Myrtaceae). Brunonia 7:277–288.
512 https://doi.org/10.1071/bru9840277

513 Barranco D, Arroyo J, Santos-Gally R (2019). Avoiding sexual interference: herkogamy and
514 dichogamy in style dimorphic flowers of *Narcissus broussonetii* (Amaryllidaceae),
515 AoB PLANTS 11 (4):plz038. https://doi.org/10.1093/aobpla/plz038

516 Barrett SC, Colautti RI, Eckert CG (2008) Plant reproductive systems and evolution during
517 biological invasion. Molecular ecology 17:373–383

518 Barrett SC, Cole WW, Herrera CM (2004) Mating patterns and genetic diversity in the wild
519 daffodil *Narcissus longispathus* (Amaryllidaceae). Heredity 92:459–465

Barrett SCH (2019) ‘A most complex marriage arrangement’: recent advances on heterostyly and unresolved questions. New Phytologist 224:1051–1067. https://doi.org/10.1111/nph.16026

Barrett SCH, Cruzan MB (1994) Incompatibility in heterostylous plants. In: Williams EG, Clarke AE, Knox RB (eds) Genetic control of self-incompatibility and reproductive development in flowering plants. Springer Netherlands, Dordrecht, pp 189–219

Barrett SCH, Shore JS (2008) New insights on heterostyly: comparative biology, ecology and genetics. In: Self-incompatibility in flowering plants. Springer Berlin Heidelberg, Berlin, Heidelberg, pp 3–32

Baskorowati L, Moncur MW, Cunningham SA, et al (2010) Reproductive biology of *Melaleuca alternifolia* (Myrtaceae) 2. Incompatibility and pollen transfer in relation to the breeding system. Aust J Bot 58:384–391. https://doi.org/10.1071/BT10036

Beardsell DV, Knox RB, Williams EG (1993) Breeding system and reproductive success of *Thryptomene calycina* (Myrtaceae). Aust J Bot 41:333–353. https://doi.org/10.1071/bt9930333

Bertin RI, Barnes C, Guttman SI (1989) Self-sterility and cryptic self-fertility in *Campsis radicans* (Bignoniaceae). Botanical Gazette 150:397–403. https://doi.org/10.1086/337785

Besnard, G, Cheptou, P-O, Debbaoui, M, et al. Paternity tests support a diallelic self-incompatibility system in a wild olive (*Olea europaea* subsp. *laperrinei*, Oleaceae). Ecology and Evolution 10:1876– 1888. https://doi.org/10.1002/ece3.5993

Busch JW, Schoen DJ (2008) The evolution of self-incompatibility when mates are limiting. Trends in Plant Science 13:128–136. https://doi.org/10.1016/j.tplants.2008.01.002

Charlesworth D, Vekemans X, Castric V, Glémin S (2005) Plant self-incompatibility systems: a molecular evolutionary perspective: research review. New Phytologist 168:61–69. https://doi.org/10.1111/j.1469-8137.2005.01443.x

Chen X, Hao S, Wang L, et al (2012) Late-acting self-incompatibility in tea plant (*Camellia sinensis*). Biologia 67:347–351. https://doi.org/10.2478/s11756-012-0018-9

Cheptou P-O (2012) Clarifying Baker's law. Annals of botany 109:633–641

Cohen JI (2010) "A case to which no parallel exists": The influence of Darwin's Different Forms of Flowers. American Journal of Botany 97:701–716. https://doi.org/10.3732/ajb.0900395

Dandelot S (2004) Les *Ludwigia* spp. invasives du Sud de la France : historique, biosystématique, biologie et écologie. Université d'Aix-Marseille

Darwin C (1877) The different forms of flowers on plants of the same species. D. Appleton

De Cauwer I, Vernet P, Billiard S, Godé C, Bourceaux A, Ponitzki C, Saumitou-Laprade P (2021) Widespread coexistence of self-compatible and self-incompatible phenotypes in a diallelic self-incompatibility system in *Ligustrum vulgare* (Oleaceae). Heredity 127**:**384–392. https://doi.org/10.1038/s41437-021-00463-4

De Nettancourt D (1997) Incompatibility in angiosperms. Sexual Plant Reproduction 10:185–199. https://doi.org/10.1007/s004970050087

561 Dickinson HG, Crabbe MJC, Gaude T (1992) Sporophytic self-incompatibility systems: S-
562 gene products. International Review of Cytology 140:525–561.
563 https://doi.org/10.1016/S0074-7696(08)61108-0

564 Dulberger R (1964) Flower dimorphism and self-incompatibility in *Narcissus tazetta* L.
565 Evolution 18:361–363. https://doi.org/10.2307/2406347

566 Dulberger R (1992) Floral polymorphisms and their functional significance in the
567 heterostylous syndrome. In: Barrett SCH (ed) Evolution and function of heterostyly.
568 Springer, Berlin, Heidelberg, pp 41–84

569 Dulberger R, Heslop-Harrison J, Lewis D (1975) Intermorph structural differences between
570 stigmatic papillae and pollen grains in relation to incompatibility in Plumbaginaceae.
571 Proceedings of the Royal Society of London Series B Biological Sciences 188:257–
572 274. https://doi.org/10.1098/rspb.1975.0018

573 Duminil J, Fineschi S, Hampe A, et al (2007) Can population genetic structure be predicted
574 from life-history traits? The American Naturalist 169:662–672

575 Ellegren H, Galtier N (2016) Determinants of genetic diversity. Nature Reviews Genetics
576 17:422–433. https://doi.org/10.1038/nrg.2016.58

577 Emerson S (1939) A Preliminary Survey of the Oenothera Organensis Population. Genetics
578 24:524–537

579 EPPO, 2011. Dutartre MA, CEMAGREF F, Secretariat E, Brunel MS (2011) Pest risk
580 analysis for: *Ludwigia grandiflora*. EPPO

581 Eyde RH (1977) Reproductive structures and evolution in *Ludwigia* (Onagraceae). I.
582 Androecium, placentation, merism. Annals of the Missouri Botanical Garden 644–655

583 Ferrer MM, Good SV (2012) Self-sterility in flowering plants: preventing self-fertilization
584 increases family diversification rates. Annals of Botany 110:535–553.
585 https://doi.org/10.1093/aob/mcs124

586 Finatto T, Dos Santos KL, Steiner N, et al (2011) Late-acting self-incompatibility in *Acca*
587 *sellowiana* (Myrtaceae) 1. Australian journal of botany 59:53–60

588 Fujii S, Kubo K, Takayama S (2016) Non-self- and self-recognition models in plant self-
589 incompatibility. Nature Plants 2:16130. https://doi.org/10.1038/nplants.2016.130

590 Genitoni J, Vassaux D, Delaunay A, Citerne S, Portillo Lemus L, Etienne M-P, Renault D,
591 Stoeckel S, Barloy D and Maury S (2020), Hypomethylation of the aquatic invasive
592 plant, *Ludwigia grandiflora subsp. hexapetala* mimics the adaptive transition into the
593 terrestrial morphotype. Physiologia Plantarum, 170: 280-298.
594 https://doi.org/10.1111/ppl.13162

595 Gibbs PE (2014) Late-acting self-incompatibility - the pariah breeding system in flowering
596 plants. New Phytologist 203:717–734. https://doi.org/10.1111/nph.12874

597 Gibbs PE, Bianchi M (1993) Post-pollination events in species of *Chorisia* (Bombacaceae)
598 and *Tabebuia* (Bignoniaceae) with late-acting self-incompatibility. Botanica Acta
599 106:64–71. https://doi.org/10.1111/j.1438-8677.1993.tb00339.x

600 Gibbs PE, Bryan GW (1986) Reproductive failure in populations of the dog-whelk, N*ucella*
601 *Lapillus*, caused by imposex induced by tributyltin from antifouling paints. Journal of
602 the Marine Biological Association of the United Kingdom 66:767–777.
603 https://doi.org/10.1017/S0025315400048414

604 Goodwillie C, Weber JJ (2018) The best of both worlds? A review of delayed selfing in
605 flowering plants. American Journal of Botany 105:641–655

606 Grossenbacher DL, Brandvain Y, Auld JR, et al (2017) Self-compatibility is over-represented
607 on islands. New Phytol 215:469–478. https://doi.org/10.1111/nph.14534

608 Hao Y-Q, Zhao X-F, She D-Y, et al (2012) The role of late-acting self-incompatibility and
609 early-acting inbreeding depression in governing female fertility in Monkshood,
610 *Aconitum kusnezoffii*. PLOS ONE 7:e47034.
611 https://doi.org/10.1371/journal.pone.0047034

612 Hieda S, Kaneko Y, Nakagawa M, Noma N (2020) *Ludwigia grandiflora* (Michx.) Greuter &
613 Burdet *subsp. hexapetala* (Hook. & Arn.) GL Nesom & Kartesz, an invasive aquatic
614 plant in Lake Biwa, the largest lake in Japan. Acta Phytotaxonomica et Geobotanica
615 71:65–71

616 Hinata K, Watanabe M, Toriyama K, Isogai A (1993) A review of recent studies on
617 homomorphic self-incompatibility. International Review of Cytology 143:257–296.
618 https://doi.org/10.1016/S0074-7696(08)61877-X

619 Igic B, Lande R, Kohn JR (2008) Loss of self-incompatibility and its evolutionary
620 consequences. International Journal of Plant Sciences 169:93–104.
621 https://doi.org/10.1086/523362

622 Kao TH, McCubbin AG (1996) How flowering plants discriminate between self and non-self
623 pollen to prevent inbreeding. PNAS 93:12059–12065

624 Kenrick J, Kaul V, Williams EG (1986) Self-incompatibility in *Acacia Retinodes*: site of
625 pollen-tube arrest is the nucellus. Planta 169(2):245–50.
626 http://www.jstor.org/stable/23378114.

627 Kerbs B, Crawford DJ, White G, et al (2020) How rapidly do self-compatible populations
628 evolve selfing? Mating system estimation within recently evolved self-compatible
629 populations of Azorean Tolpis succulenta (Asteraceae). Ecology and Evolution
630 10:13990–13999. https://doi.org/10.1002/ece3.6992

631 Liao T, Yuan D-Y, Zou F, et al (2014) Self-sterility in *Camellia oleifera* may be due to the
632 prezygotic late-acting self-incompatibility. PLoS One 9:e99639

633 Lloyd DG (1992) Self- and Cross-Fertilization in Plants. II. The Selection of Self-
634 Fertilization. International Journal of Plant Sciences 153:370–380.
635 https://doi.org/10.1086/297041

636 Martin FW (1959) Staining and observing pollen tubes in the style by means of fluorescence.
637 Stain Technology 34(3):125-128. https://doi.org/10.3109/10520295909114663

638 Matsui K, Yasui Y (2020). Buckwheat heteromorphic self-incompatibility: genetics,
639 genomics and application to breeding. Breeding science 70(1):32–38.
640 https://doi.org/10.1270/jsbbs.19083

641 Medrano M, Requerey R, Karron JD, Herrera CM (2012) Herkogamy and mate diversity in
642 the wild daffodil Narcissus longispathus: beyond the selfing–outcrossing paradigm in
643 the evolution of mixed mating. Plant Biology 14:801–810

644 Nesom GL, Kartesz JT (2000) Observations on the Ludwigia uruguayensis Complex
645 (Onagraceae) in the United States. Castanea 65:123–125

646 Oliveira P, Gibbs P (1994) Pollination biology and breeding systems of six Vochysia species
647 (Vochysiaceae) in Central Brazil. Journal of Tropical Ecology 509–522

648 Opedal OH (2018) Herkogamy, a Principal Functional Trait of Plant Reproductive Biology.
649 International Journal of Plant Sciences 179(9):677-687.
650 https://doi.org/10.1086/700314

651 Portillo-Lemus LO, Bozec M, Harang M, et al (2021) Self-incompatibility limits sexual
652 reproduction rather than environmental conditions in an invasive water primrose.
653 Plant-Environment Interactions 2:74–86. https://doi.org/10.1002/pei3.10042

654 Pound LM, Wallwork MAB, Potts BM, Sedgley M (2002) Self-incompatibility in Eucalyptus
655 globulus ssp. globulus (Myrtaceae). Australian Journal of Botany 50:365–372

656 Rangappa Thimmaiah M, Choudhary SB, Sharma HK, et al (2018) Late-acting self-
657 incompatibility: a barrier to self-fertilization in sunnhemp (Crotalaria juncea L.).
658 Euphytica 214:19. https://doi.org/10.1007/s10681-017-2096-9

659 Raven PH (1979) A survey of reproductive biology in Onagraceae. New Zealand Journal of
660 Botany 17:575–593. https://doi.org/10.1080/0028825X.1979.10432572

661 Razanajatovo M, Maurel N, Dawson W, et al (2016) Plants capable of selfing are more likely
662 to become naturalized. Nature communications 7:1–9

663 Rigakishi MI (1918) Studies on the Embryo Sac and Fertilization in Oenothera. Annals of
664 Botany 279–318

665 Ruane LG, Mangum SM, Horner KM, Moeller DA (2020) The opportunity for outcrossing
666 varies across the geographic range of the primarily selfing Clarkia xantiana ssp.

parviflora. American Journal of Botany 107:1198–1207. https://doi.org/10.1002/ajb2.1510

Ruaux B (2008) Les plantes envahissantes des corridors fluviaux: traits biologiques, impacts de *Ludwigia peploides* et *L. grandiflora* en Loire moyenne et implications pour la gestion. Université François Rabelais

Safavian D, Shore JS (2010) Structure of styles and pollen tubes of distylous Turnera joelii and T. scabra (Turneraceae): are there different mechanisms of incompatibility between the morphs? Sexual plant reproduction 23:225–237

Sage TL, Bertin RI, Williams EG (1994) Ovarian and other late-acting self-incompatibility systems. In: Williams EG, Clarke AE, Knox RB (eds) Genetic control of self-incompatibility and reproductive development in flowering plants. Springer Netherlands, Dordrecht, pp 116–140

Sage TL, Price MV, Waser NM (2006) Self-sterility in Ipomopsis aggregata (Polemoniaceae) is due to prezygotic ovule degeneration. American Journal of Botany 93:254–262. https://doi.org/10.3732/ajb.93.2.254

Sage TL, Strumas F, Cole WW, Barrett SCH (1999) Differential ovule development following self- and cross-pollination: the basis of self-sterility in Narcissus triandrus (Amaryllidaceae). American Journal of Botany 86:855–870. https://doi.org/10.2307/2656706

Sakai WS. Simple method for differential staining of paraffin embedded plant material using toluidine blue o. Stain Technol. 1973 Sep;48(5):247-9. doi: 10.3109/10520297309116632.

Sakai S (1995) Evolutionarily Stable Selfing Rates of Hermaphroditic Plants in Competing and Delayed Selfing Modes with Allocation to Attractive Structures. Evolution 49:557–564. https://doi.org/10.1111/j.1558-5646.1995.tb02287.x

Santos-Gally R, Gonzalez-Voyer A, Arroyo J (2013) Deconstructing Heterostyly: The Evolutionary Role of Incompatibility System, Pollinators, and Floral Architecture. Evolution 67:2072–2082. https://doi.org/10.1111/evo.12087

Seavey SR, Bawa KS (1986) Late-acting self-incompatibility in angiosperms. Bot Rev 52:195–219. https://doi.org/10.1007/BF02861001

Seavey SR, Carter SK (1996) Ovule fates in Epilobium obcordatum (Onagraceae). American Journal of Botany 83:316–325. https://doi.org/10.1002/j.1537-2197.1996.tb12712.x

Shimizu KK, Tsuchimatsu T (2015) Evolution of selfing: recurrent patterns in molecular adaptation. Annual Review of Ecology, Evolution, and Systematics 46:593–622

Simon-Porcar VI, de Castro A, Herrero M, Arroyo J (2015) Ovarian self-incompatibility in Narcissus papyraceus (Amaryllidaceae) is the result of a pre-zygotic response. Botanical Journal of the Linnean Society 177:629–643

Takayama S, Isogai A (2005) Self-incompatibility in plants. Annu Rev Plant Biol 56:467–489. https://doi.org/10.1146/annurev.arplant.56.032604.144249

Thouvenot L, Haury J, Thiebaut G (2013) A success story: water primroses, aquatic plant pests. Aquatic Conservation: Marine and Freshwater Ecosystems 23:790–803

Tilquin JP, de Brouwer K (1982) Aspects cytologiques de la reproduction sexuée dans le genre Fuchsia. Bulletin de la Société Royale de Botanique de Belgique/Bulletin van de Koninklijke Belgische Botanische Vereniging 33–42

711 Tobe H, Raven PH (1986) A comparative study of the embryology of Ludwigia
712 (Onagraceae): characteristics, variation, and relationships. Annals of the Missouri
713 Botanical Garden 768–787

714 Vaughton G, Ramsey M, Johnson SD (2010) Pollination and late-acting self-incompatibility
715 in Cyrtanthus breviflorus (Amaryllidaceae): implications for seed production. Annals
716 of Botany 106:547–555. https://doi.org/10.1093/aob/mcq149

717 Webb CJ, Lloyd DJ (1986) The avoidance of interference between the presentation of pollen
718 and stigmas in angiosperms II. Herkogamy. New Zealand Journal of Botany
719 24(1):163-178, https://doi.org/10.1080/0028825X.1986.10409726

720 Xu K (2021) The coevolution of flower longevity and self-fertilization in hermaphroditic
721 plants. Evolution n/a: https://doi.org/10.1111/evo.14303

722 Zhou W, Barrett SCH, Wang H, Li D-Z (2015) Reciprocal herkogamy promotes
723 disassortative mating in a distylous species with intramorph compatibility. New
724 Phytologist 206:1503–1512. https://doi.org/10.1111/nph.13326

Figures and Support information

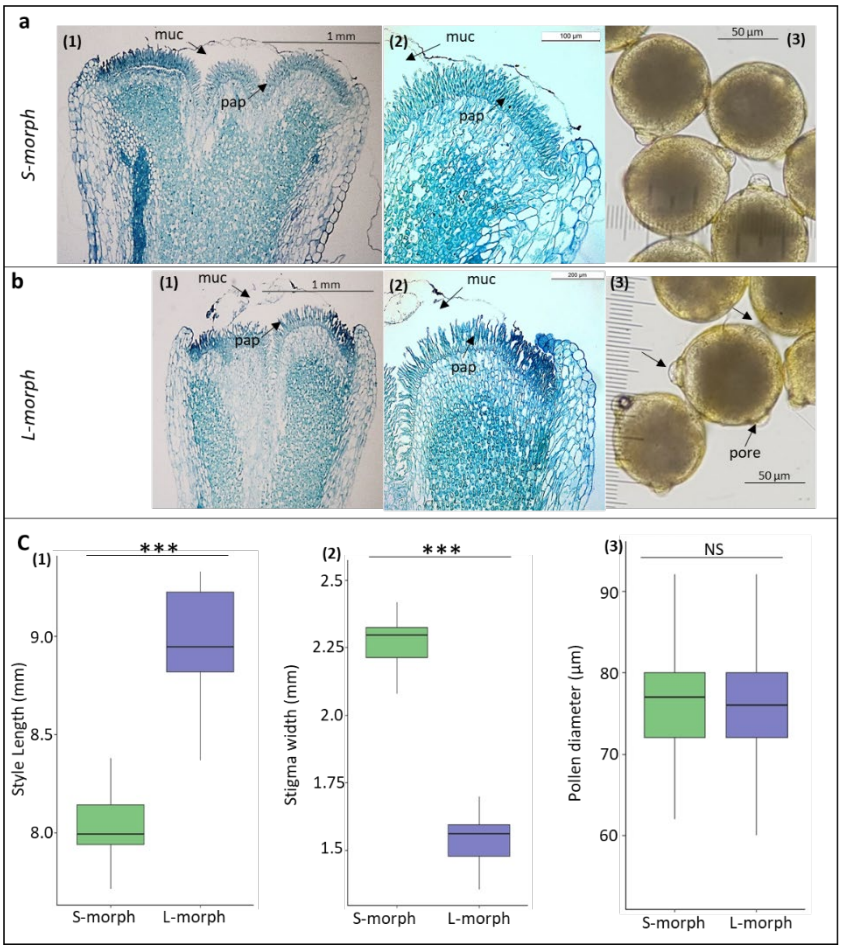

Figure 1: Stigma and pollen morphologies in both floral morphs of *Ludwigia grandiflora* subsp. *hexapetala*.

- Stigma section of S-morph (a 1, 2) and L-morph (b 1, 2) under the 10x (a1, b1) and 20x (a2, b1) objectives of optic microscope stained with toluidine blue O. Stigma sections of the stigma have a thickness of 15 µm. In both floral morphs, the stigma was filled with mucilage (mu) (a1-2, b1-2,). Both floral morphs showed the same shape of stigmatic papillae (pap).

- Pollen morphologies of S-morph (a3) and L-morph (b3) under 20X objective of optical microscope. Both morphotypes shared the same shape and size of pollen (a3, b3) and the same diameter of pollen (c3).

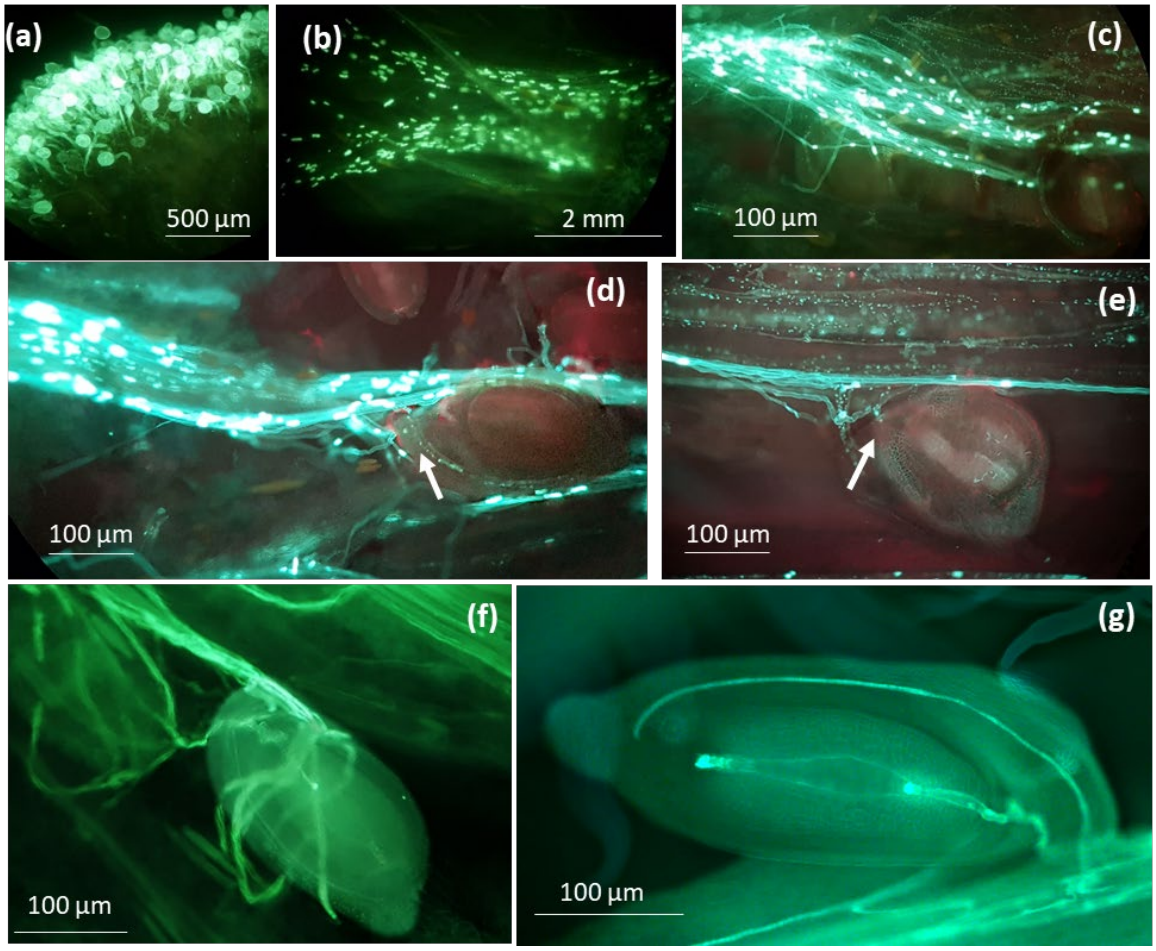

Figure 2: Fluorescence aniline blue staining of self-pollen tube in L-morph pistils (a-f).

a) Pollen grains germination on a stigma surface (zoom 10X); b) Pollen tubes elongating in a style (zoom 2.5X); c, d, e) Pollen tubes in the ovarian area (zoom 20X); f) Pollen tubes in the area of embryo sac (noticed for 6 pollen tubes over 300 studied). g) Pollen tubes in the area of embryo sac in S-morph ovary after self-pollination.

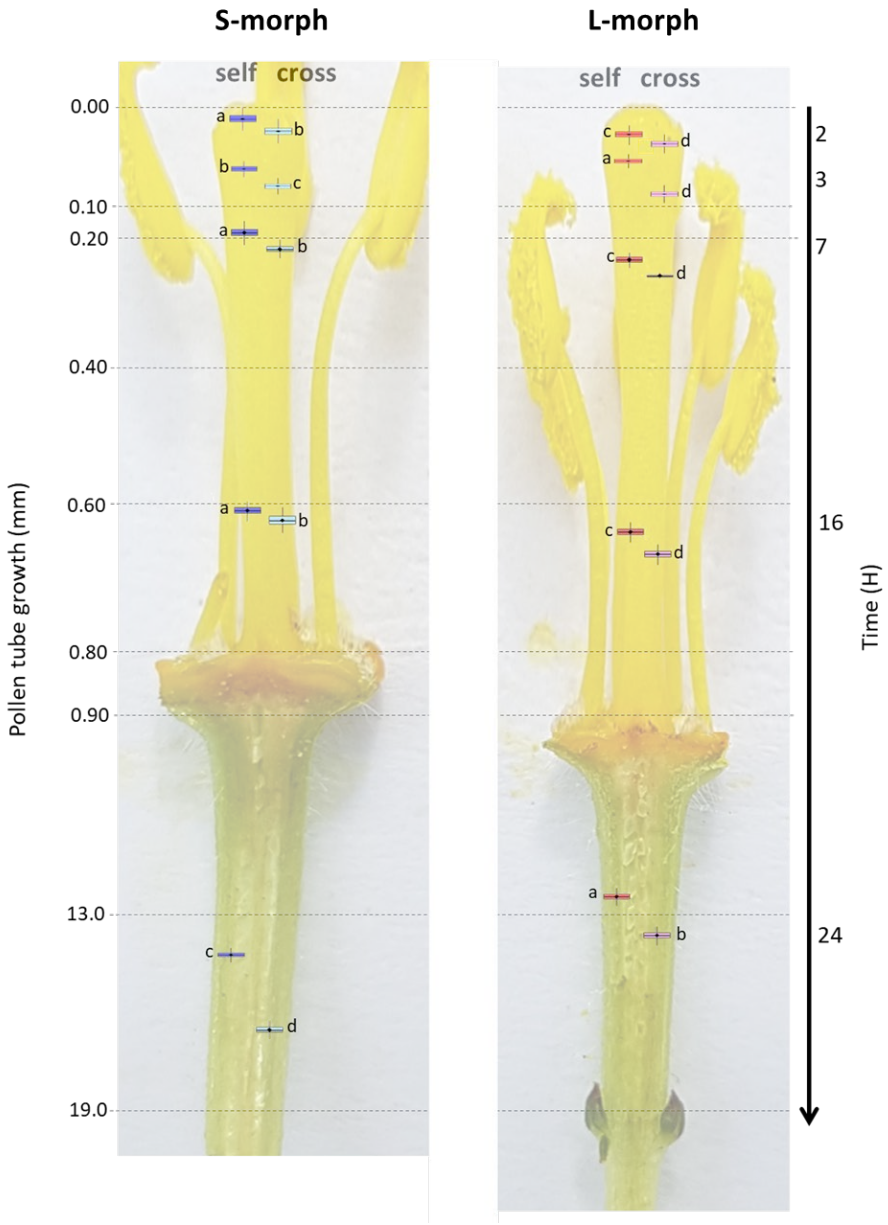

Figure 3: Kinetic of pollen tube elongations in both floral morphs in *Ludwigia grandiflora* subsp. *hexapetala*.

a) Kinetic of pollen tube elongations in S-morph styles when self- and cross-pollinated (left, blue and sky-blue boxes respectively); b) Kinetic of pollen tube elongations in L-morph style when self- and cross-pollinated (right, red and pink boxes respectively). Significance letters were obtained using a Tukey's honestly significant difference (HSD) post-hoc comparisons of the means. In both floral morphs, cross-pollen tubes elongated faster than self-pollen.

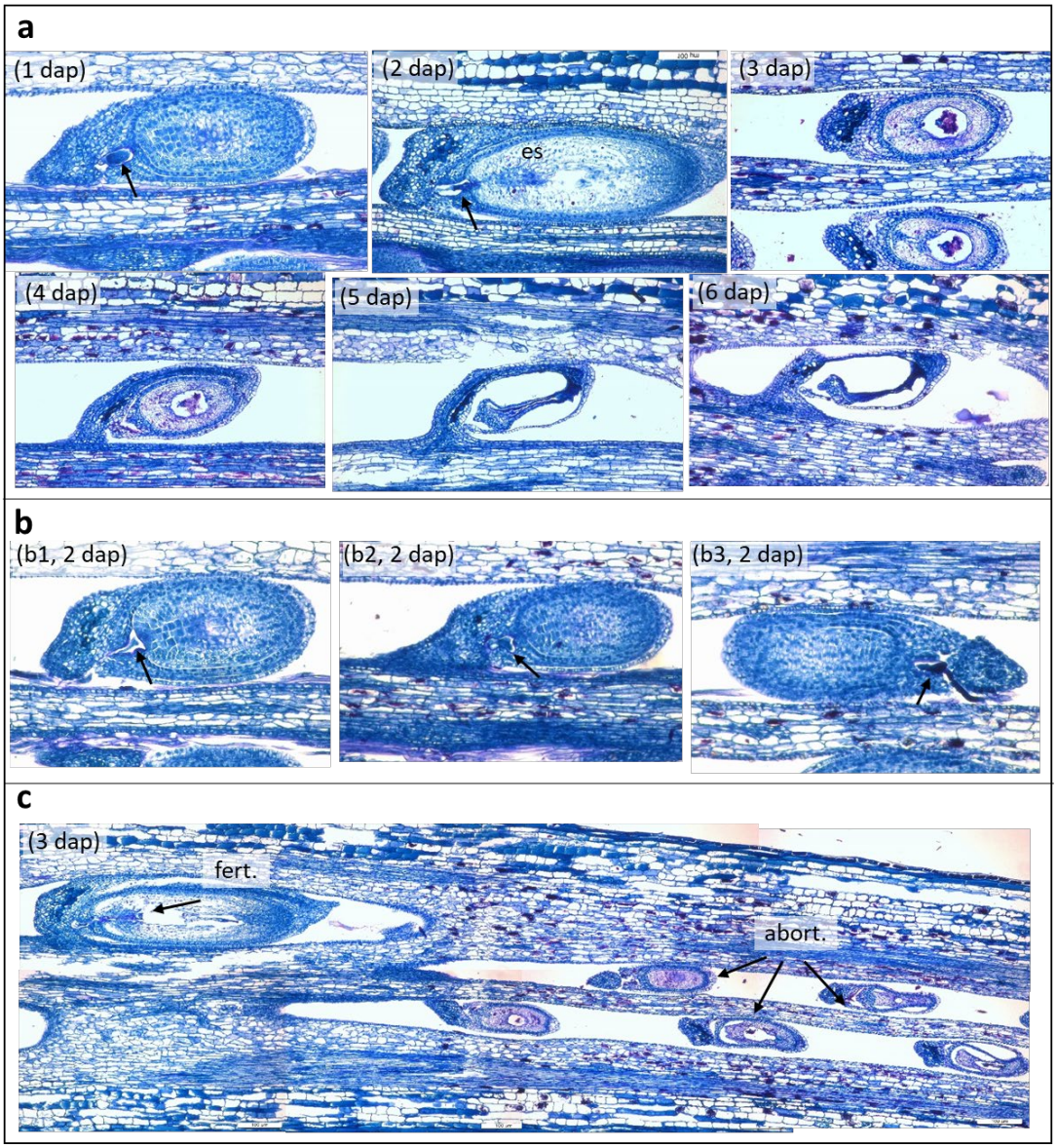

Figure 4: Temporal evolution of embryo sacs, ovules and ovaries in self-incompatible L-morph flowers after self-pollination. a) Abortive ovules sections after 1, 2, 3, 5 and 6 days after self-pollination (dap); b) Self-pollen tubes that stopped their elongations two days after self-pollination (dap) in three different ovules (1 to 3). The arrows indicate the tips of the self-pollen tube stopped between the ovarian tissues and the beginning of the first cell layers of the ovule integuments (see figure 5a for a comprehensive representation of the ovule parts); c) Example of a rare self-fertilisation event (fert.) obtained three days after self-pollination (dap) informing the "small fruit" formation. Only ~0.33% ovules were fertilised (1/300 ovules observations)

761 (fertilisation = fert; abortive ovules= abort). All sections stained with toluidine blue O (zoom

762 10X). See figure 5 a comprehensive representation of the ovule parts.

763

764

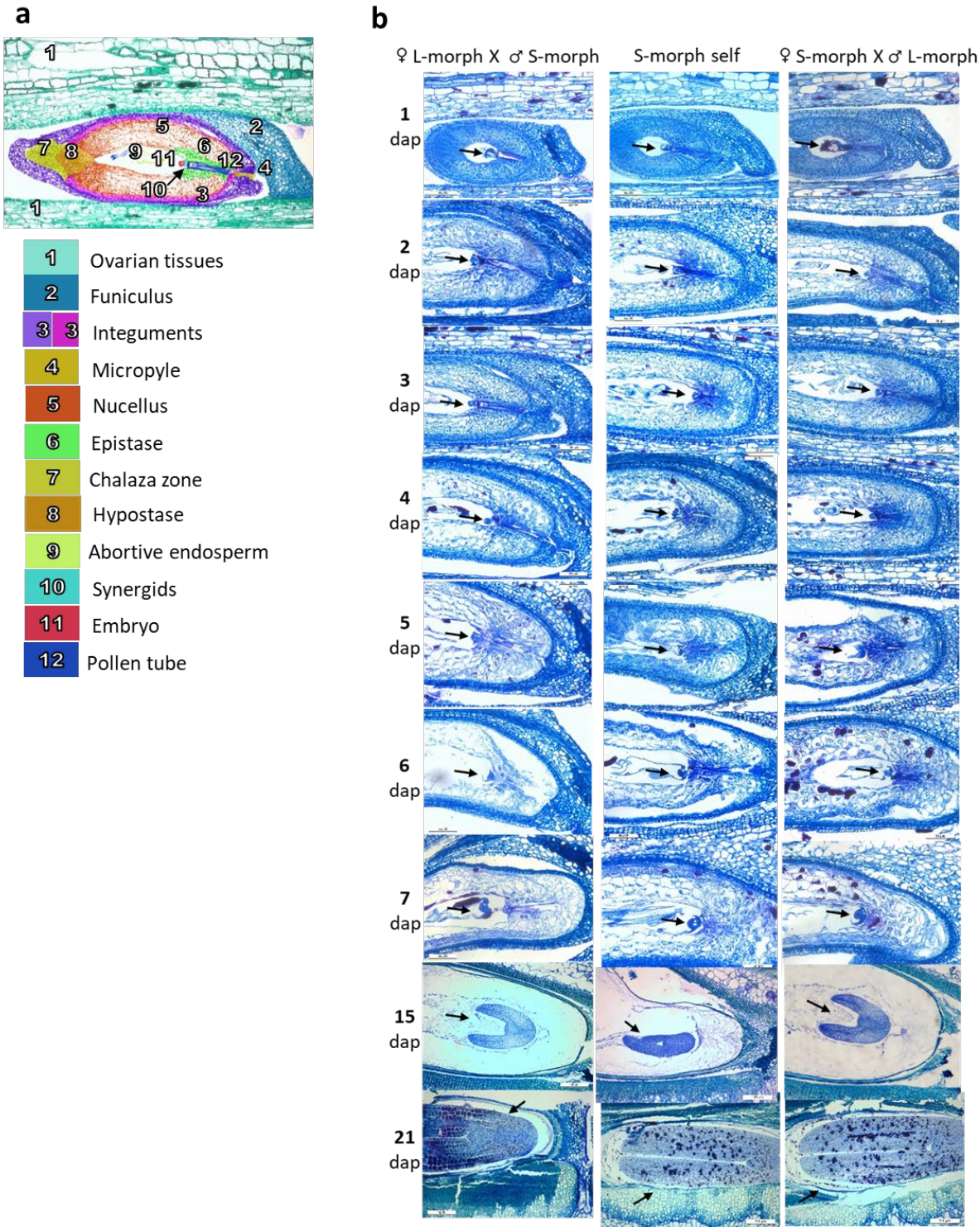

765

766 **Figure 5:** Fertilisation and embryonic development after cross and self-pollinating the self-

767 incompatible L-morph and the self-compatible S-morph flowers.

768 a - A comprehensive, colorized scheme of the different tissue parts of a L-morph ovule 3 days
769 after disassortative pollination.

770 b- Evolution of the ovules 1, 2, 3, 4, 5, 6, 7, 15, and 21 days after pollen deposition on the
771 stigmas (dap): (1) L-morph ovules after cross-pollination (♀ L-m X ♂ S-m); (2) S-morph ovules
772 after self-pollination; (3) S-morph ovules after cross-pollination (♀ S-m X ♂ L-m).

773 The arrows indicate the development of embryo. All sections were stained with toluidine blue
774 O, 20X zoom under optical microscope.

775

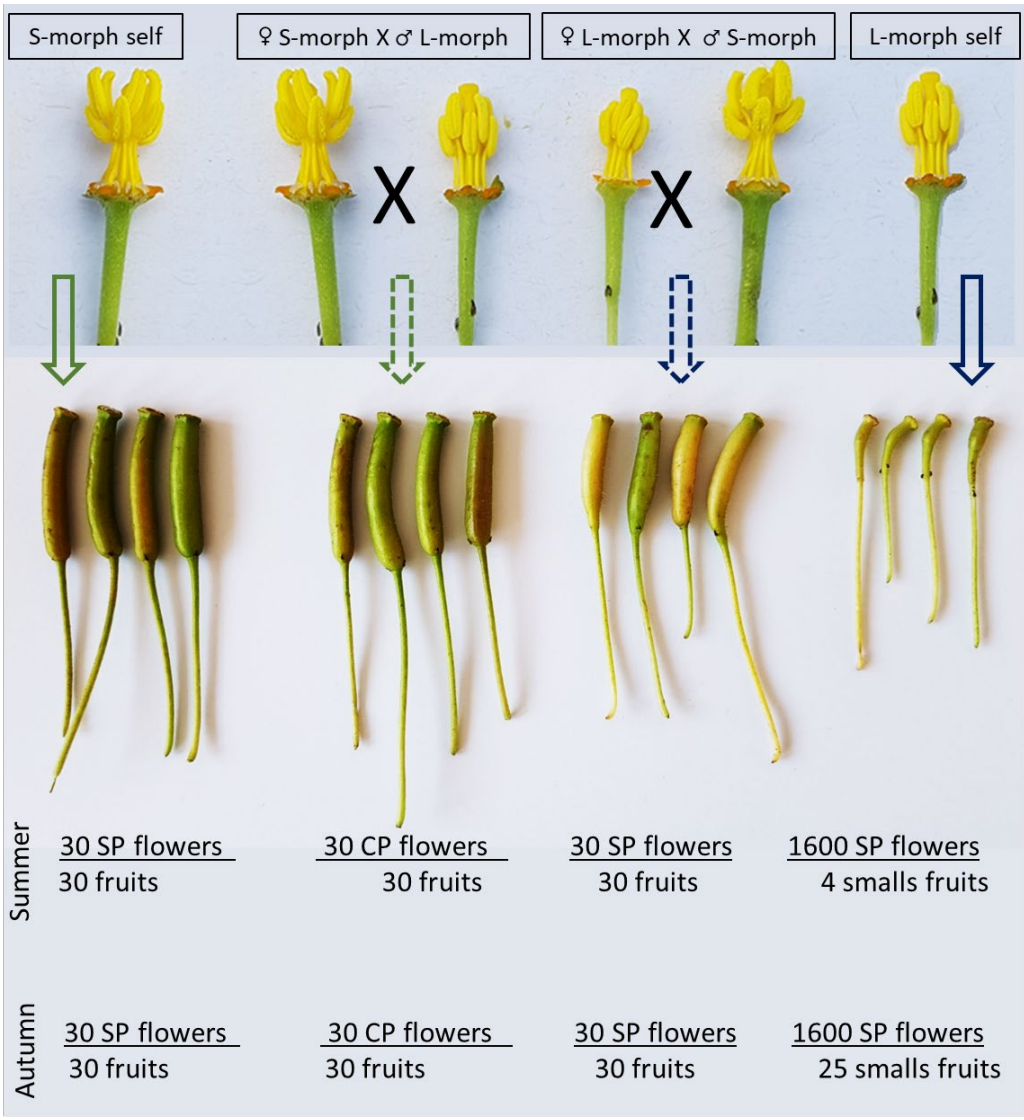

Figure 6: Summary of the fruit-set obtained from S-morph and L-morph flowers after hand-controlled pollination (SP = Self-pollination; CP = Cross-pollination) in summer and autumn.

- All S-morph flowers produced fully-seeded fruits, in summer and autumn, both after self- and cross-pollinations.

- All L-morph flowers produced fully-seeded fruits, in summer and autumn, when pollinated with S-morph pollen (L-morph x S-morph).

- 0.25% and 1.56% of L-morph flowers produced “small fruits” in summer and autumn when self-pollinated. These “small fruits” contained one to nine seeds that all successfully germinated and grew into viable seedlings.

Table S1: Fruit-set, seed-set and germination rate in five S-morph and five L-morph monomorphic *in natura* populations in western Europe.

Fruit-set, seed-set and mean number of seeds produced in the studied *in natura* monomorphic populations of *Lgh*. Seed-set productions per m^2 in monomorphic S-morph populations were estimated by counting the number of seeds produced by fruits in 5 quadrats of $1m^2$ and multiplied by the mean number of counted fruits per quadrat. Seed-set productions per quadrat in L-morph populations are reported as the exhaustive number of seeds within all the fruits found in the quadrat.

Population	GPS Location	Floral morph	Mean number of seeds per fruit	Fruit-set per m^2	Seed-set per m^2	Germination percentage
Chambéon	45°41'03.4"N 4°12'12.1"E	L	4.18	22	92	95.67%
Châtel-de-Neuvre	46°24'05.4"N 3°19'10.1"E	L	6.40	15	96	93.75%
Gilly-sur-Loire	46°31'40.6"N 3°48'25.7"E	L	6.79	28	190	93.68%
Pouilly-sur-Loire	47°16'48.4"N 2°57'25.2"E	L	5.68	19	108	89.81%
Orléans	47°53'41.3"N 1°55'48.6"E	L	6.20	35	217	94.47%
Pont-de-Cé	47°25'40.7"N 0°31'28.9"W	S	55	792	43560	90.30%
Mazerolles	47°23'17.3"N 1°28'07.4"W	S	60	864	51840	96.71%
Saint-Aignan-sur-Cher	47°16'19.8"N 1°22'32.1"E	S	55	528	29040	89.46%
Lac-de-Maine	47°27'34.7"N 0°35'30.8"W	S	50	624	31200	98.12%
Sabot-d'Or	47°19'14.1"N 2°15'24.4"W	S	50	384	19200	91.55%

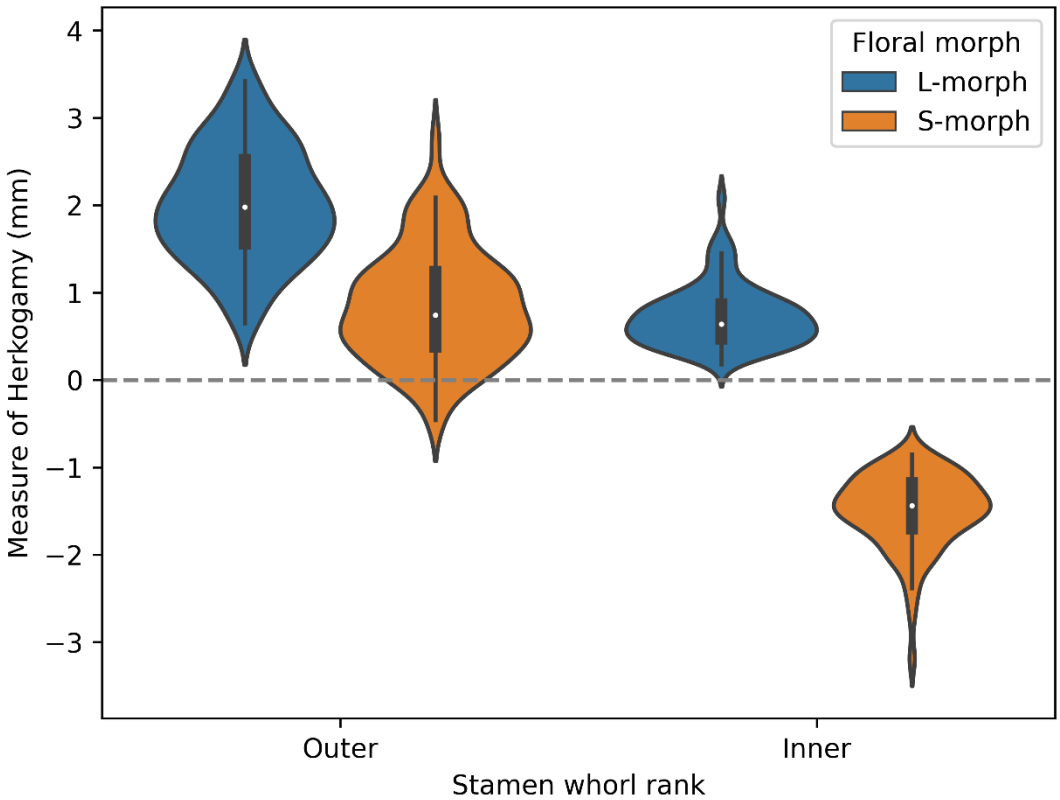

L-morph flower showing approach herkogamy S-morph flower showing reverse herkogamy

Figure S1: Measures and photos of herkogamy in self-incompatible L-morph and self-compatible S-morph flowers found in Western European populations of *Lgh*.

Measures are reported for the outer and inner whorls of anthers. 150 measured flowers per violin plot, 5 populations sampled across the Loire watershed per morph.

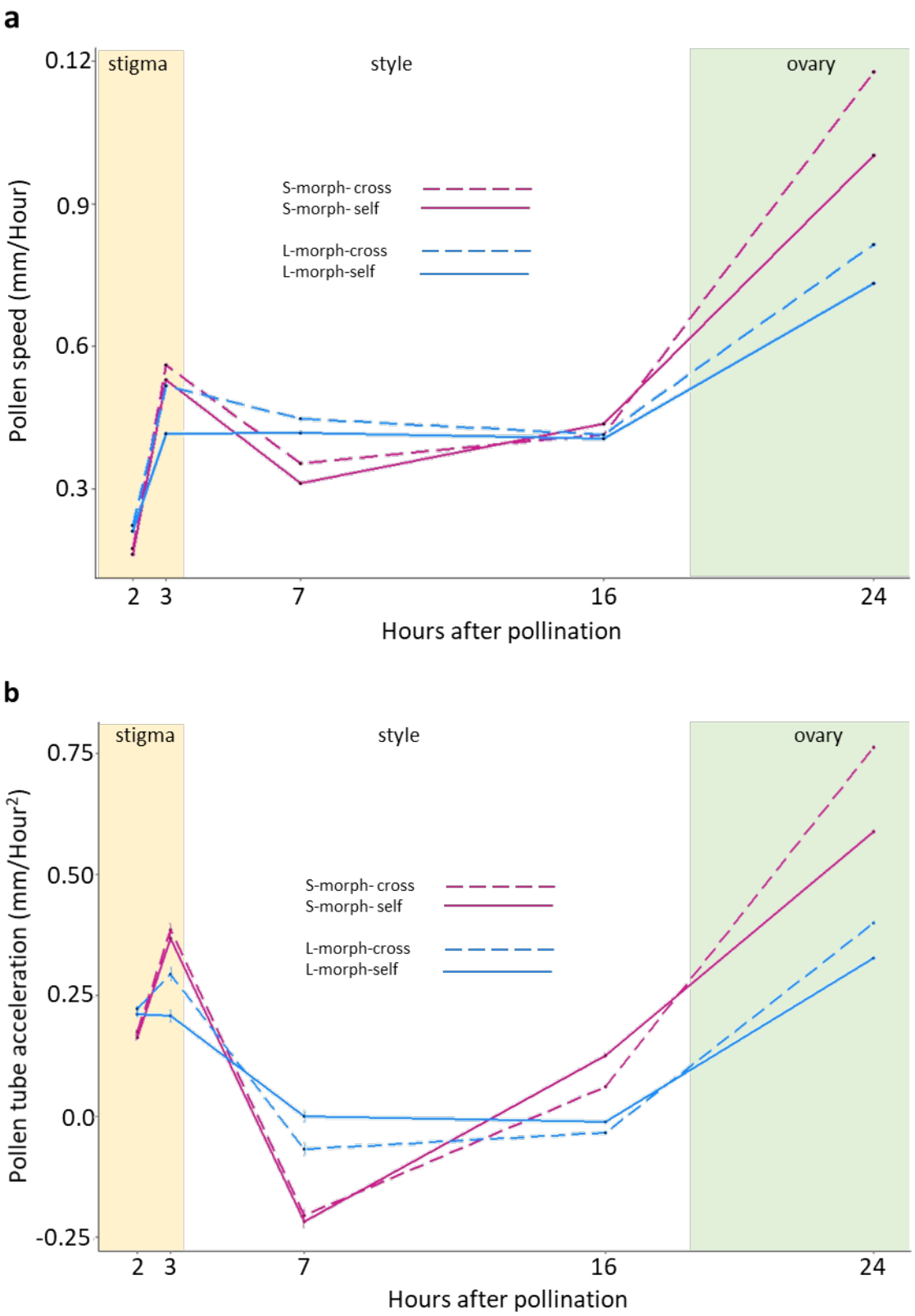

Figure S2: Speed and acceleration of pollen tube elongations in both floral morphs in *Ludwigia grandiflora* subsp. *hexapetala* after self- and cross-pollinated.

Red = S-morph, blue = L-morph; solid line = self-pollination (self) and dotted line=cross-pollination (cross). a) Speed of pollen tube elongations in both S-morph and L-morph styles after self and cross pollinations. b) Acceleration of pollen tube elongations in both S-morph and L-morph styles after self and cross pollinations.

Table S2: Analyses of the variations of pollen tube elongation along time (a), speed (b) and acceleration of pollen tube elongation (b) in both floral morphs in *Ludwigia grandiflora* subsp. *hexapetala* after self- and cross-pollinations.

(a)

Analysis of Variance Table
Response: Growth of pollen tubes => anova(lm(Length ~ Pollination_condition * Hours_after_pollinations))

Anova Table (Type III tests)

	Df	Sum_Sq	Mean_Sq	F_value	Pr(>F)
Pollination_conditions	3	1.94571	0.64857	6094	< 2.2e-16 ***
Residuals	796	0.08472	0.00011		
Pollination_conditions	3	1.89545	0.63182	4700.7	< 2.2e-16 ***
Residuals	796	0.10699	0.00013		
Pollination_conditions	3	46.067	15.3558	80721	< 2.2e-16 ***
Residuals	796	0.151	0.0002		
Pollination_conditions	3	26.1592	8.7197	65513	< 2.2e-16 ***
Residuals	796	0.1059	0.0001		
Pollination_conditions	3	1315.28	438.43	3306413	< 2.2e-16 ***
Residuals	796	0.11	0		

Significance codes: .001 "***"; .01 "**"; .05 "*"; non significant "NS."

Analysis of Variance Table
Tukey test; alpha = 0.05
Response: length of pollen tubes

Pollination_conditions	HAP	mean	SD	groups of signif
S-morph_self	2	0.3251328	0.0102478	a
S-morph x L-morph	2	0.349352	0.0099562	b
L-morph_self	2	0.4207731	0.0103041	c
L-morph x S-morph	2	0.4449497	0.0106426	d
S-morph_self	3	0.8550793	0.0103665	b
S-morph x L-morph	3	0.909661	0.0124761	c
L-morph_self	3	0.8374607	0.0101908	a
L-morph x S-morph	3	0.9615144	0.0129607	d
S-morph_self	7	2.1001969	0.0163765	a
S-morph x L-morph	7	2.3251743	0.0136882	b
L-morph_self	7	2.5056041	0.0113881	c
L-morph x S-morph	7	2.7542894	0.0131105	d
S-morph_self	16	6.0289593	0.0117017	a
S-morph x L-morph	16	6.0539117	0.0136438	b
L-morph_self	16	6.1577877	0.0098296	c
L-morph x S-morph	16	6.4826446	0.0104896	d
S-morph_self	24	14.0489390	0.0099906	c
S-morph x L-morph	24	15.4732020	0.0099158	d
L-morph_self	24	12.01793	0.0130931	a
L-morph x S-morph	24	12.9937810	0.0125769	b

Signif. codes: a -> b -> c -> d = p-value <2.2e-16

(b)

```
Analysis of Variance Table
Response: speed of pollen tubes =>  anova(lm(speed ~ Pollination_condition))
```

Anova Table (Type III tests)

	Df	Sum_Sq	Mean_Sq	F_value	Pr(>F)
Pollination_conditions	3	0.48643	0.162142	6094	< 2.2e-16 ***
Residuals	796	0.02118	0.000027		
Pollination_conditions	3	2.26998	0.75666	5629.5	< 2.2e-16 ***
Residuals	796	0.10699	0.00013		
Pollination_conditions	3	2.30357	0.76786	64582	< 2.2e-16 ***
Residuals	796	0.00946	0.00001		
Pollination_conditions	3	0.104195	0.034732	21137	< 2.2e-16 ***
Residuals	796	0.001308	0.000002		
Pollination_conditions	3	23.7891	7.9297	3827337	< 2.2e-16 ***
Residuals	796	0.0016	0		

Significance codes: .001 "***"; .01 "**"; .05 "*"; non significant "NS."

Analysis of Variance Table
Tukey test; alpha = 0.05
Response: Speed of pollen tubes

Pollination_conditions	HAP	mean	SD	groups of signif
morph-S_self	2	0.1625664	0.0051239	d
morph-S x morph-L	2	0.174676	0.0049781	c
morph-L_self	2	0.2103866	0.005152	b
morph-L x morph-S	2	0.2224748	0.0053213	a
morph-S_self	3	0.5298404	0.0103665	b
morph-S x morph-L	3	0.559422	0.0124761	a
morph-L_self	3	0.4176024	0.0101908	d
morph-L x morph-S	3	0.5166561	0.0129607	c
morph-S_self	7	0.3109203	0.0040941	d
morph-S x morph-L	7	0.3534147	0.0034221	c
morph-L_self	7	0.417389	0.002847	b
morph-L x morph-S	7	0.4483104	0.0032776	a
morph-S_self	16	0.4366003	0.0013002	a
morph-S x morph-L	16	0.4143728	0.001516	b
morph-L_self	16	0.4057916	0.0010922	c
morph-L x morph-S	16	0.4143976	0.0011655	b
morph-S_self	24	1.0024951	0.0012488	b
morph-S x morph-L	24	1.177403	0.0012395	a
morph-L_self	24	0.7325065	0.0016366	d
morph-L x morph-S	24	0.8138629	0.0015721	c

Signif. codes: a -> b -> c -> d = P value <2.2e-16

(c)

```
Analysis of Variance Table
Response: accelleration of pollen tubes =>  anova(lm(acceleration~
Pollination_condition ))
```

Anova Table (Type III tests)

	Df	Sum_Sq	Mean_Sq	F_value	Pr(>F)
Pollination_conditions	3	1.94571	0.64857	6094	< 2.2e-16 ***
Residuals	796	0.08472	0.00011		
Pollination_conditions	3	1.89545	0.63182	4700.7	< 2.2e-16 ***
Residuals	796	0.10699	0.00013		
Pollination_conditions	3	46.067	15.3558	80721	< 2.2e-16 ***
Residuals	796	0.151	0.0002		
Pollination_conditions	3	26.1592	8.7197	65513	< 2.2e-16 ***
Residuals	796	0.1059	0.0001		
Pollination_conditions	3	1315.28	438.43	3306413	< 2.2e-16 ***
Residuals	796	0.11	0		

Significance codes: .001 "***"; .01 "**"; .05 "*"; non significant "NS."

Analysis of Variance Table
Tukey test; alpha = 0.05
Response: acceleration of pollen tubes

Pollination_conditions	HAP	mean	SD	groups of signif
morph-S_self	2	0.1625664	0.0051239	d
morph-S x morph-L	2	0.174676	0.0049781	c
morph-L_self	2	0.2103866	0.005152	b
morph-L x morph-S	2	0.2224748	0.0053213	a
morph-S_self	3	0.3672739	0.0112325	b
morph-S x morph-L	3	0.384746	0.0129094	a
morph-L_self	3	0.2072158	0.0116108	d
morph-L x morph-S	3	0.2941812	0.0137249	c
morph-S_self	7	-0.21892	0.0107856	d
morph-S x morph-L	7	-0.206007	0.0131338	c
morph-L_self	7	-0.000213	0.0106224	a
morph-L x morph-S	7	-0.068346	0.0132985	b
morph-S_self	16	0.12568	0.0044317	a
morph-S x morph-L	16	0.0609581	0.0038266	b
morph-L_self	16	-0.011597	0.0029275	c
morph-L x morph-S	16	-0.033913	0.0034387	d
morph-S_self	24	0.5880975	0.0016601	b
morph-S x morph-L	24	0.7630302	0.0019039	a
morph-L_self	24	0.3267149	0.0018812	d
morph-L x morph-S	24	0.3994653	0.0019593	c

Signif. codes: a -> b -> c -> d = P value <2.2e-16

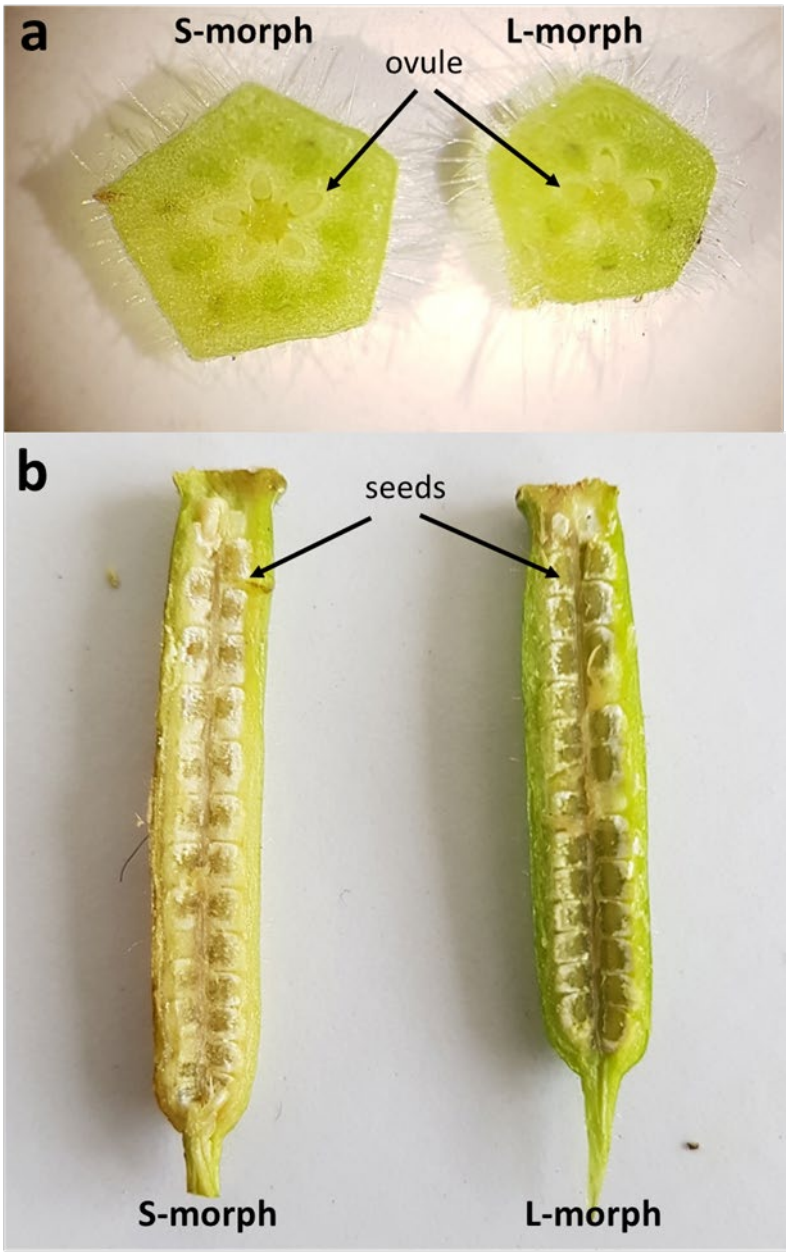

Figure S3: a) transversal and b) longitudinal sections of petaloculate ovary from 5-merous floral morphs of *Ludwigia grandiflora* subsp. *hexapetala*.